Research Square

Preprints are preliminary reports that have not undergone peer review.
They should not be considered conclusive, used to inform clinical practice,
or referenced by the media as validated information.

Integrating Crop Growth Models and Genomic Prediction to Improve Flowering Time Forecasting Across Novel Environments and Breeding Lines

Melanie Cabrera
University of Florida
Lance Baker
University of Florida
Diego Jarquin
University of Florida
Eduardo Vallejos
University of Florida
Carlos Messina
cmessina@ufl.edu
University of Florida

Research Article

Keywords: crop growth model, genomic selection, GxExM, flowering time, CGM-WGP, horticultural crops

Posted Date: July 14th, 2026

DOI: https://doi.org/10.21203/rs.3.rs-9890445/v1

License: This work is licensed under a Creative Commons Attribution 4.0 International License.
Read Full License

Additional Declarations: No competing interests reported.

Integrating Crop Growth Models and Genomic Prediction to Improve Flowering Time Forecasting Across Novel Environments and Breeding Lines

Melanie Cabrera (0009-0001-4086-8870)[1], Lance J. Baker (0009-0009-2031-9290) [1], Diego Jarquin (0000-0002-5098-2060) [2], C. Eduardo Vallejos (0000-0001-8936-7885) [1], Carlos D. Messina (0000-0002-5501-9281) [1,*]

[1] Horticultural Sciences Department, IFAS, University of Florida, Gainesville, Florida, USA

[2]Agronomy Department, IFAS, University of Florida, Gainesville, Florida, USA

* Corresponding author: Carlos D Messina (cmessina@ufl.edu) 2550 Hull Rd, Gainesville, FL, 32611, USA

Abstract

Genomic selection has accelerated genetic gain in many breeding programs worldwide but genotype-by-environment-by-management (GxExM) hampers further progress for systems where these interactions are important and not well represented in the training data. Process-based crop growth models (CGMs), which encode physiological relationships between plants and their environments, can extrapolate to novel conditions but cannot directly leverage genomic information. Coupling these complementary approaches in the Crop Growth Model–Whole Genome Prediction (CGM-WGP) framework addresses both limitations, yet applications in horticultural crops remain scarce. In this study, we apply CGM-WGP to predict flowering time in broccoli (*Brassica oleracea* var. *italica*) and common bean (*Phaseolus vulgaris* L.), two horticultural species with contrasting physiological responses to temperature and photoperiod. Genotype-specific thermal time requirements and photoperiod parameters were jointly estimated with genome-wide marker effects and predictions were compared against a Reaction Norm Genomic Best Linear Unbiased Prediction (RN-GBLUP) benchmark across four cross-validation scenarios of increasing predictive difficulty. RN-GBLUP achieved the highest accuracy under sparse-testing scenarios where training data covered all target environments, while CGM-WGP outperformed RN-GBLUP when predicting untested environments and untested genotype-environment combinations (broccoli: Pearson $r = 0.66$, RMSE = 9.4 days; bean: $r = 0.86$, RMSE = 5.2 days). These results demonstrate that CGM-WGP can be applied to horticultural crops using genome-wide markers alone, but without requiring prior identification of quantitative trait loci. CGM-WGP also provides a modular foundation that can be extended to predict the timing of other developmental transitions and output traits such as biomass and yield.

Keywords: crop growth model; genomic selection; GxExM; flowering time; CGM-WGP; horticultural crops

Key Message

The CGM-WGP framework is generalizable as demonstrated for two horticultural crops with contrasting physiology and different from prior research.

Author Contributions

MC: Methodology, Investigation, Conceptualization, Writing; LJB: Software; DJ: Review & Editing; CEV: Methodology, Writing; CDM: Methodology, Conceptualization, Software, Writing; Supervision

1. Introduction

As computing power increases and genomic platforms become faster and more affordable, plant breeders have increasingly explored how genomic information can be leveraged to accelerate genetic gain. Genomic selection (GS) is broadly defined as the use of genome-wide DNA markers to predict the performance of individuals that have not yet been phenotypically evaluated (Meuwissen et al. 2001; Bernardo and Yu 2007; Heffner et al. 2009). GS has gained widespread adoption and is now being implemented in breeding programs across a range of species (Alemu et al. 2024; Beyene et al. 2015; Dreisigacker et al. 2023). GS help breeders realize high on-farm genetic gain when training and prediction populations are closely related and when the multienvironment trials (MET) is highly correlated with the target population of environment (TPE, Cooper and Messina, 2023). However, its predictive power deteriorates when applied to novel environments, particularly those characterized by strong genotype-by-environment-by-management (GxExM) interactions that were not present in the training data.

This challenge of limited predictability has motivated the development of prediction frameworks that couple mechanistic crop models with genomic prediction to achieve greater flexibility under environmental novelty (Messina et al. 2018; Cooper et al. 2016; Technow et al. 2015). Process-based crop models, commonly referred to as crop growth models (CGMs), represent the integration of physiological processes driven by environmental inputs such as temperature, photoperiod, solar radiation, water, and nitrogen (Jones et al. 2003; Holzworth et al. 2014). Because these models encode known physiological relationships between the plant and its environment, genotype-specific parameters estimated from CGMs can harness prior scientific knowledge to predict performance of genotypes into environments not yet observed. However,

CGMs are not designed to leverage the genomic information increasingly available in modern breeding programs—the common practice is to calibrate each genotype in multiple environments.

Improved phenotype prediction across an environmental range can be attained by combining a mechanistic model, which defines how environmental and management factors shape growth and development, with a genomic model capturing the genetic factors governing the relevant physiological responses. This integration is known in the literature as Crop Growth Model-Whole Genome Prediction (CGM-WGP, Technow et al. 2015; Cooper et al. 2016; Messina et al. 2018). Although CGM-WGP is not a new concept, it has continued to evolve over the past decade, with some of the most successful applications in row crops such as maize (Messina et al. 2018; Diepenbrock et al., 2022; Messina et al., 2025) demonstrating improved prediction under drought stress and high GxExM interactions, and more generally with increasing complexity of the GxExM system (Messina et al., 2023b; Messina et al., 2025). Despite this progress, CGM-WGP has not yet been applied to horticultural crops, where comparatively smaller breeding programs and greater environmental diversity make efficient prediction tools particularly valuable.

In this study, we apply the CGM-WGP framework to predict flowering time in two horticultural species: broccoli (*Brassica oleracea* var. *italica*) and common bean (*Phaseolus vulgaris* L.). Broccoli is a nutritionally dense temperate vegetable whose cultivation is constrained by its sensitivity to high temperatures, limiting production in tropical and subtropical regions where diet-related micronutrient deficiencies are most prevalent (Cabrera and Messina 2025). Expanding production into these new, unexplored environments requires identifying and

breeding heat tolerant germplasm that will enable breeding of tropical and subtropical cultivars. Yet, the infrastructure needed to evaluate genetic material under the target growing conditions is often absent in the very regions where the crop could have the greatest nutritional impact. Common bean is a widely consumed tropical legume and important global protein source, included here as a complementary species to assess the generality of the framework and its known photoperiod response. Together, the two species present contrasting population development strategies, different physiological responses to temperature and photoperiod, and distinct experimental designs, providing a rigorous test of whether CGM-WGP can generalize across horticultural crops.

Time to flowering, measured as days to first anthesis from planting (DAP), is the focal trait for both species due to its impact on yield. In broccoli, time to flowering governs marketable yield directly because the commercially harvested organ is the immature inflorescence. Consensus in the literature indicates that head development and flowering time are highly temperature-sensitive (Siomos et al. 2022), with head formation ceasing above 23-24°C in many cultivars (Lin et al. 2019; Farnham and Bjorkman 2011) and inflorescence development arrested altogether under prolonged temperatures above 30°C in others (Björkman and Pearson 1998). Genotype-dependent responses are also well documented, including increases in the minimum number of leaves and delayed head initiation under high temperature conditions (Lindemann-Zutz et al. 2016; Olesen and Grevsen 1997; Wurr et al. 1995; Lin et al. 2018). While photoperiod research on broccoli is sparse, existing studies show no significant effect on head initiation or flowering time, with temperature being the primary driver of development in modern cultivars (Tan et al. 2000b; Tan et al. 2000a). In beans, yield and quality are directly related to time to flowering which is heavily influenced by both photoperiod and temperature (Peksen

2007; Monterroso and Wien 1990). Pod and seed numbers are markedly reduced by exposure to high temperatures at anthesis due to increased abscission of flower buds, flowers, and young pods, and by failure of fertilization and seed development (Ofir et al. 1993). Photoperiod plays a critical role, with approximately 60% of bean genotypes reported to be photoperiod sensitive (White and Laing 1989).

Despite the agronomic importance of predicting time to flowering across diverse environments, existing modeling efforts for both broccoli and bean have been largely context specific, reflecting the production systems and environments in which they were developed. For broccoli, Tan et al. (2000a) established foundational thermal time models from field experiments in subtropical southeast Queensland. Subsequent studies extended these approaches to predict head initiation dates and yield in broccoli grown throughout Scotland (Cammarano et al. 2020). Others have calibrated models to European growing conditions (Lindemann-Zutz et al. 2016) and integrated management optimization for California's coastal production zones (Kim et al. 2021). Across these efforts, a common limitation is that each model was parameterized for the climatic and cultivar context in which it was built, with limited evidence of transferability to novel environments or untested germplasm.

For common bean, modeling efforts have been more extensive. The CSM-CROPGRO-Dry Bean within the DSSAT ecosystem (Hoogenboom et al. 2004), represent the most widely used process-based tools and have been applied to irrigation management and yield prediction across diverse production systems. More recently, a series of increasingly sophisticated QTL-based dynamic models have been developed using the same dataset employed here. Bhakta et al. (2017) established a foundational predictive model for time to flowering with a bi-parental

recombinant inbred family using 12 QTL across five environmentally distinct sites. Wallach et al. (2018) extended this model by proposing a dynamic model in which three parameters of a temperature and photoperiod driven development model are expressed as linear functions of QTL capturing GxE interaction. Most recently, Vallejos et al. (2022) further refined this framework using a mixed-effects model with separate minimum and maximum temperature inputs, epistatic QTL interactions, and an unstructured residual covariance across sites. While these QTL-based approaches represent meaningful advances, they share a fundamental limitation, that is the development of QTL models that are often restricted to the founder populations. Leveraging genome-wide marker data directly to predict flowering time in new genotypes drawn from diverse germplasm can increase the applicability of beans models, a limitation that becomes particularly consequential when the trait's genetic architecture is polygenic. The objectives of this study were to: (i) develop a CGM-WGP framework to predict time to flowering in horticultural crops using genome-wide marker data; and (ii) to evaluate prediction accuracy over other statistical model across novel genotypes and untested environments.

2. Materials and Methods

2.1 Plant Material and Experimental Design

2.1.1 Broccoli

This project was carried out with the immortal BolTBDH doubled haploid (DH) biparental population (supplementary Figure 1), derived from a cross between double haploid parental lines 'TO1000DH3' (P1; *Brassica oleracea* var. *alboglabra*) and 'Early Big' (P2; *B. oleracea* var.

italica) (Iniguez-Luy et al. 2009). A single F_1 was selfed, and 200 DH lines generated via anther culture. Seeds were from USDA-ARS in Geneva, NY, and sown into 200-cell trays filled with commercial potting mix (Fafard 3B; Conrad Fafard Inc., Agawam, MA) on six separate dates: July 24, 2023; October 20, 2023; January 30, 2024; July 22, 2024; October 21, 2024; and March 7, 2025. These dates were chosen to span a natural temperature gradient from early to late season conditions in North Florida.

Broccoli seedlings were grown in a climate-controlled greenhouse at Speedling Inc., Ruskin, FL, for six weeks. Afterward, they were transplanted to a field in Hastings, FL, on six corresponding dates: September 8, 2023; December 6, 2023; March 15, 2024; September 17, 2024; December 3, 2024; and April 14, 2025. Transplanting was done onto raised beds covered with white plastic mulch and equipped with two drip irrigation lines to ensure optimal water distribution. Standard regional practices for fertilization and irrigation were followed, along with integrated pest management protocols to control pests and diseases.

2.1.2 Beans

A recombinant inbred line (RIL) population of 187 genotypes was developed from a cross between the determinate Andean cultivar Calima and the indeterminate Mesoamerican cultivar Jamapa via single-seed descent to the F11 generation, followed by bulking to the F14 generation (further details in Bhakta et al. 2015). Population structure is shown in supplementary Figure 2. The population was evaluated across five environments: Citra, FL, USA (CT; March–June 2011), Palmira, Colombia (PA; November 2011–January 2012), Popayán, Colombia (PO; March–June 2012), Isabela, Puerto Rico (PR; February–May 2012), and Prosper, North Dakota,

USA (ND; May–August 2012). Full details of the experimental design are provided by Bhakta et al. (2017).

2.2 Phenotyping for time to flowering

Broccoli plants were monitored weekly for flowering time and were considered to be flowering when distinct flower structures appeared, including expanded yellow or white petals, consistent with other published methodologies (Okazaki et al. 2007; Camargo and Osborn 1996; Shu et al. 2018; Stansell et al. 2019). Days to flowering were then calculated by subtracting the planting date from the flowering date. Similarly, flowering time in beans was recorded as number of days it took for 50% of the plants in the same plot to reach anthesis.

2.3 Environmental Data

Daily weather data for the broccoli experiment were accessed from the Hastings weather station of the Florida Automated Weather Network (FAWN). Daily temperature and solar radiation data were downloaded for the six planting dates. Weather data for the bean experiments were obtained from (Vallejos et al. 2022; Wallach et al. 2018; Bhakta et al. 2017).

2.4 Crop Growth Models: Mechanistic Component

Time to flowering was modeled as a thermal time driven process governed by a cardinal temperature beta function (Eq. 1) and photoperiod function (Eq. 2). The cardinal function describes the relative rate of development as a response to daily mean temperature, parameterized by the base (T_b), optimum (T_{opt}), and ceiling (T_c) temperatures, with the shape controlled by two dimensionless parameters, α and β:

$$f(T) = \begin{cases} \left(\frac{T-T_b}{T_{opt}-T_b}\right)^{\alpha} \left(\frac{T_c-T}{T_c-T_{opt}}\right)^{\beta}, & T_b < T < T_c \\ 0, & otherwise \end{cases} \quad \text{(Eq. 1)}$$

The function $f(T)$ represents the relative thermal response, scaling between 0 and 1 with a maximum at T_{opt}, and is subsequently scaled by the genotype-specific physiological time requirement Θ_g to yield the daily development rate. The effect of daylength on daily development rate was modeled with the following photoperiod function:

$$\psi_{e,t}(P_{c,g}) = \begin{cases} DL_{e,t} - P_{c,g}, & DL_{e,t} > P_{c,g} \\ P_{c,g} - DL_{e,t}, & DL_{e,t} < P_{c,g} \\ 0, & otherwise \end{cases} \quad \text{(Eq. 2)}$$

where $DL_{e,t}$ is the daylength in hours on day *t* in environment *e,* $P_{c,g}$ is the critical photoperiod for genotype *g.* The daily development rate $R_{g,e,t}$ for genotype *g* in environment *e* on day *t* combines the thermal response with the additive photoperiod penalty, scaled by a genotype-specific thermal requirement Θ_g:

$$R_{g,e,t} = \begin{cases} \frac{1}{\Theta_g}\,(f(T_{e,t}) - S_g \cdot \psi_{e,t}), & f(T_{e,t}) > S_g \cdot \psi_{e,t} \\ 0, & otherwise \end{cases} \quad \text{(Eq. 3)}$$

where S_g is a genotype-specific rate penalty per hour of deviation. Under this parameterization, $S_g = 0$ reduces the model to a thermal-only accumulator; $S_g > 0$ imposes a slowdown whenever the daily photoperiod differs from the genotype-specific critical value in the unfavorable direction. Flowering was predicted as the day on which cumulative development first reached completion, defined as the day d when the sum of daily development rates satisfies:

$$\widehat{DAP}_{g,e} = min\left\{d: \sum_{t=1}^{d} R_{g,e,t} \geq 1\right\} \quad \text{(Eq. 4)}$$

The parameter Θ_g therefore represents the genotype-specific physiological time requirement to flowering, with larger values corresponding to later-flowering genotypes that require greater accumulated photothermal development to reach anthesis. The estimation of Θ_g across genotypes and its connection to genomic information is described in the following section.

2.5 Whole-Genome Prediction: Genomic Component

Genomic information was incorporated into the model through the genotype-specific physiological time requirement Θ_g, which serves as the bridge between the mechanistic crop model and the genomic prediction component. A genomic relationship matrix $\boldsymbol{G}$ was constructed for each crop from genome-wide SNP markers obtained through genotype-by-sequencing, using the AGHmatrix R package (Amadeu et al. 2023) following VanRaden's method (VanRaden 2008):

$$\boldsymbol{G} = \frac{\boldsymbol{Z}\boldsymbol{Z}^T}{2\sum p_j(1-p_j)} \quad \text{(Eq. 5)}$$

where $\boldsymbol{Z}$ is the centered marker matrix and p_j is the allele frequency at locus *j*. The G-matrix serves as the covariance structure for the genomic prior placed on Θ_g, assumed to follow a multivariate normal distribution:

$$\Theta \sim N(\mu_\Theta 1,\ \sigma^2_\Theta G) \quad \text{(Eq. 6)}$$

Where μ_Θ is the population mean-physiological time requirement and σ^2_Θ is the genomic variance component. This prior shrinks individual Θ_g estimates toward genetically similar genotypes, regularizing the solution and enabling genomic prediction for new genotypes not observed in any

training environment. Analogous genomic priors were placed on S_g and $P_{c,g}$, their behavior under the available data is reported in Section 3.2.

2.6 Coupling of Crop Growth Models with Whole-Genome Prediction

An Expectation-Maximization (EM) algorithm (Dempster et al. 1977) was used to alternate between updating the population-level hyperparameters ($\mu_\Theta,\ \sigma^2_\Theta$) and optimizing the genotype-level parameters ($\Theta_g, S_g, P_{c,g}$) jointly across all genotypes via L-BFGS-B, a limited memory quasi-Newton method suited to large-scale bounded optimization (Byrd et al. 1995). The EM alternates between two steps until convergence. The E-step updates the genomic prior hyperparameters ($\mu_\Theta,\ \sigma^2_\Theta$) from current per-genotype estimates, and an M-step re-optimizes ($\Theta_g, S_g, P_{c,g}$) via L-BFGS-B under the updated prior. CGM and genomic components were estimated using standard WGP algorithm that builds upon the original approach proposed by Messina et al. (2006):

$$\mathcal{L} = \underbrace{\sum_{g,e}\left(\widehat{DAP}_{g,e} - DAP^{obs}_{g,e}\right)^2}_{SSE} + \underbrace{\sum_k \frac{1}{\sigma^2_k}(\boldsymbol{\theta}_k - \mu_k\mathbf{1})^T\,\boldsymbol{G}^{-1}(\boldsymbol{\theta}_k - \mu_k\mathbf{1})}_{Genomic\ prior} + \underbrace{n_g \sum_k ln\ \sigma^2_k}_{Log-Det} \qquad \text{(Eq. 7)}$$

where $k \in \{\Theta, S, P_c\}$ indexes the three genotype-level parameter vectors, each regularized by a genomic prior with covariance $\sigma^2_k G$, and n_g is the number of genotypes. Prediction for new genotypes not observed during training was performed using genomic best linear unbiased prediction (GBLUP):

$$\widehat{\Theta}_n = \mu_\Theta + \boldsymbol{G}_{n,t}\boldsymbol{G}^{-1}_{t,t}(\boldsymbol{\Theta}_t - \mu_\Theta\mathbf{1}) \qquad \text{(Eq. 8)}$$

where $\boldsymbol{G}_{n,t}$ is the submatrix of genomic relationships between new and training genotypes. This equation leverages the genetic relatedness between a new genotype and all training genotypes to borrow information proportional to genomic similarity, enabling prediction for lines that were never phenotyped. The architecture of the full model is illustrated in Figure 2.

2.7 Baseline Models

2.7.1 Reaction Norm GBLUP (RN-GBLUP)

We fit an extended RN-GBLUP model for the genomic prediction of flowering time to incorporate interactions between markers and the environments following the framework of Jarquín et al. (2014):

$$y_{ijk} = \mu + w_{ij} + p_{ij} + g_j + gw_{ij} + pg_{ij} + \varepsilon_{ijk} \qquad \text{(Eq. 9)}$$

with $w \sim N\,(0, \Omega_T \sigma_w^2)$, $p \sim N\,(0, \Omega_{DL} \sigma_p^2)$, $g \sim N\,(0, G\sigma_g^2)$, $gw \sim N(0, [Z_g G Z'_g] \circ \Omega_T {\sigma^2}_{gw})$, $pg \sim N(0, [Z_g G Z'_g] \circ \Omega_{DL} {\sigma^2}_{pg})$, $\varepsilon_{ijk} \underset{\sim}{^{IID}} N\,(0, \sigma_\varepsilon^2)$. The $\boldsymbol{G}$ matrix is the genomic relationship matrix derived from markers, $\boldsymbol{\Omega_T}$ is the environmental covariance matrix constructed from temperature, and $\boldsymbol{\Omega_{DL}}$ is the environmental covariance matrix constructed from daylength. Both $\boldsymbol{\Omega}$ matrices capture environmental similarity across planting dates and locations, allowing the model to borrow information across environments in proportion to their thermal and photoperiod similarity, respectively. The Hadamard product $\circ$ between $\left[\mathrm{Z}_g \mathrm{G} \mathrm{Z}'_g\right]$ and each $\boldsymbol{\Omega}$ matrix captures genotype-specific responses to temperature and photoperiod, providing a genomic benchmark that accounts for the same environmental drivers explicitly modeled in the mechanistic component of the CGM-WGP framework.

2.7.2 Crop Growth Model

The mechanistic crop model described in Section 2.4 was used as a physiological baseline without any genomic component. A single set of population-mean parameters was estimated from the training data and applied uniformly to all genotypes, reflecting the principal limitation of purely mechanistic crop models: their inability to distinguish between genotypes without external genetic information. Prior work has addressed this by calibrating the crop model independently for each genotype (Hoogenboom et al., 2004; Messina et al., 2006; Vallejos et al. 2022); while this approach allows the model to capture genetic variability, it does so without the regularization that genome-wide marker information provides. Flowering time predictions under this formulation vary across environments through the temperature and photoperiod response functions but remain identical for all genotypes within a given environment. Differences in performance between this physiological baseline and the CGM-WGP therefore quantify the predictive value added by incorporating genomic relatedness into the mechanistic framework.

2.7.3 GBLUP

A baseline genomic model was fitted using only the genomic relationship matrix $\boldsymbol{G}$ and the fixed effect of environment. The phenotype of genotype j in environment i was modeled as:

$$y_{ijk} = \mu + e_i + g_j + \varepsilon_{ijk} \quad \text{(Eq.10)}$$

With $g \sim N\ (0, G\sigma_g^2)$ and $\varepsilon_{ijk} \underset{\sim}{^{IID}} N\ (0, \sigma_\varepsilon^2\ )$. This model captures additive genetic variation through genomic relatedness and accounts for mean differences between environments but does not model genotype-by-environment interaction. It serves as a benchmark for the predictive

value of genomic information alone, without the mechanistic environmental response of the crop growth model or the environmental covariance structure of the reaction-norm formulation.

2.8 Cross Validation Schemes

Four cross-validation schemes were implemented following Burgueño et al. (2012) and Jarquín et al. (2020) to evaluate model performance across scenarios of increasing predictive difficulty and relevance for plant breeding programs. The sparse-testing scheme (CV2) assessed performance where 20% of genotypes were randomly withheld per environment but remained observable in other training environments, simulating incomplete trial data. The new varieties scheme (CV1) evaluated prediction for completely unobserved breeding lines, where 20% of genotypes were withheld from all training environments, relying entirely on genomic relatedness for prediction. The new environment scheme (CV0) used a leave-one-environment-out approach, withholding one entire environment at a time and predicting all genotypes within it using the mechanistic model's environmental inputs. The new genotype new environment scheme (CV00) combined both sources of novelty, withholding one entire environment along with an additional 20% of genotypes per fold; this represents the most demanding scenario, in which predictions must be made for both novel genotypes and novel environments. Schemes involving random genotype splits (CV2, CV1, and the genotype component of CV00) were repeated five times with different random seeds, while environment-based folds (CV0, CV00) were deterministic, with one fold per environment. Prediction accuracy was reported as the Pearson correlation coefficient (r) and root mean square error (RMSE), averaged across repetitions.

3. Results

3.1 Phenotypic Variation in Flowering Time

Both crops exhibit environment-dependent shifts in the mean and variance of time to flowering, though the nature and magnitudes of these shifts differed substantially between species (Figure 3, supplementary Figure 3). In beans, the five environments produce a gradient of flowering time responses. PAL and PR showed relatively similar, tight distributions centered around 36 DAP, while CIT and POP showed slightly wider distributions with means ranging from 42 to 46 DAP. ND stands apart, with mean flowering time shifting to approximately 60 DAP and variance substantially greater than in PAL and PR. The higher latitude of ND slowed developmental rates, increasing both the mean and range of flowering time and revealing genetic variation in photoperiod sensitivity that is less apparent in tropical environments where daylength variation across the growing season is minimal.

In broccoli, the distributions are generally wider and more variable across plantings, reflecting the population's segregation for temperature responsiveness also referred to as heat tolerance in the literature as it is being evaluated outside its ideal environment. Plantings 1 and 4, which correspond to early-season transplanting in North Florida, produced wide distributions with long tails centered around 55 DAP. Planting 3 and 6 (late-season transplants) produced the lowest mean DAP values and the narrowest distributions, consistent with the heat susceptibility of broccoli.

3. 2 CGM-WGP Parameters Estimates

After running the CGM-WGP we extracted the per-genotype thermal-time requirements Θ_g in both beans and broccoli (Figure 4). Beans exhibited a tight distribution around the population

mean ($\mu_\Theta = 38.80, \sigma_\Theta = 2.65$), while broccoli was considerably more variable ($\mu_\Theta = 38.38, \sigma_\Theta = 5.03$). The narrow-sense heritability of Θ_g estimated by fitting a simple GBLUP to the aggregated Θ_g values across the new environment predictions, was moderate in beans ($h^2 = 0.47$) and low in broccoli ($h^2 = 0.08$). The low broccoli estimate likely reflects several factors. In part it seems from the broader phenotypic spread across the six broccoli plantings, which were staggered across a thermal gradient specifically to surface this variation. It may also be explained by the complexity of the trait itself, which encompasses both the rate of vegetative and reproductive development. Because narrow-sense heritability captures only additive genetic variance, it excludes epistatic and genotype-by-environment interactions that may contribute substantially to Θ_g.

The photoperiod parameters S_g and $P_{c,g}$ collapsed to population-mean values during the EM in both species. We interpret this as a consequence of limited day length contrast in the training environments. In the bean dataset, four near-equator to subtropical sites (2.4-29.4°N) with narrow-to-moderate photoperiod range, and in the broccoli dataset there is only one location with narrow photoperiod shifts (29.7 °N; 10.4-13.4 h). Therefore, per-genotype photoperiod sensitivity is weakly identified relative to its prior. The photoperiod response is consequently captured as a species-level effect in our data.

3. 3 Prediction Performance Across Cross-Validation Scenarios

Prediction accuracy was evaluated under the four scenarios using Pearson correlation (Table 1; Figure 5): CV2 (sparse testing), CV1 (new genotypes), CV0 (new environment), and CV00 (new genotypes and environment). Our benchmark models performed as expected, GBLUP deteriorated in scenarios where environments were held out, while the mechanistic model cannot

be applied in new genotype scenarios since it is only able to produce identical predictions for all genotypes within an environment. In contrast, CGM-WGP and RN-GBLUP performed better. RN-GBLUP was most accurate in both species when the training covered all environments like in the case of sparse-testing and new genotype scenarios; the CGM-WGP prediction was a close second. However, the rankings of these methods were reversed with CGM-WGP becoming more accurate than RN-GBLUP when the target environment was held out (in the case of new environment and new genotype and environment).

Under leave-one-environment-out prediction (Figure 6), RN-GBLUP predicts well in beans for three of the experimental sites (predictions are near the 1:1 line) but shows larger errors at the CIT and ND sites. In comparison, RN-GLUP did not predict as well in the broccoli experiments. Interestingly, the CGM-WGP method displays better predicting ability as it tracks the 1:1 line closely across the full range of flowering times in both species (beans $r = 0.86$, RMSE = 5.2 d; broccoli $r = 0.66$, RMSE = 9.4 d). Both methods accrue more errors at ND because the four training environments all span tropical to subtropical latitudes, leaving ND's temperate photoperiod regime outside the training regime, though the mechanistic component of the CGM-WGP recovers more of this extrapolated variation than the statistical kernel of the RN-GBLUP. A similar pattern holds in broccoli, where the late-season Plantings 3 and 6 were harder to predict when training was restricted to cooler plantings; here too, the mechanistic component captured more of the held-out variation than the kernel approach.

4. Discussion

4.1 Extending CGM-WGP to Horticultural Crops

This study demonstrates the generalizability of the CGM-WGP framework to horticultural crops, extending prior applications in major row crops such as maize (Messina et al. 2018; Cooper et al. 2016; Diepenbrock et al., 2022). The successful application to both broccoli and common bean, with contrasting experimental designs, population development strategies, and physiological responses to photoperiod and temperature, suggests that grounding predictions in physiological parameters and genomic relationships confers the flexibility needed to accommodate diverse horticultural and genetic systems. Importantly, we demonstrated a framework that can enable trait dissection to predict complex or emergent phenotypes (Messina et al. 2025; Hammer et al. 2019) and thus capture the diversity of paths follow by plants to express a complex trait.

A primary advantage of the CGM-WGP framework lies in its modularity. The mechanistic component is built on cardinal temperature and photoperiod parameters that are well-established for a wide range of crops and can be independently calibrated for each species without modifying the underlying model architecture. Parameters can be divided into species and genotype levels. In our case, cardinal temperatures were deemed fixed constants set prior to model fitting that capture the thermal response characteristic of the crop; at the genotype level, the model estimates genotype-specific parameters, particularly the thermal time requirement and photoperiod sensitivity, that capture heritable variation among individuals within a species. In the fitting exercise, Θ_g carried essentially all per-genotype variation, while S_g and $P_{c,g}$ collapsed to species-level means given the available daylength contrast (Sections 3.2 and 4.4). This means the same framework can be deployed across crops with varying physiological responses to temperature and photoperiod simply by calibrating the species level constants, while the genotype level estimation will be accomplished through the genomic prior. Without losing generality the routines used here to predict time to flowering could be extended to include the

timing of other developmental transitions, growth, traits underpinning water balance, and other processes until a full crop model is incorporated into the algorithm.

4.2 Structural versus statistical representations of GxE

Process-based crop models derive their predictive strength from encoding prior knowledge in the form of physiological relationships, allowing them to interpolate non-linear and complex developmental responses to environmental conditions with limited training data (Boote et al. 1996). When we fitted the mechanistic component of our framework (Section 2.7.2) without any genomic information, predictions captured environment-driven variation in time to flowering but could not differentiate among genotypes. For any given fit, all individuals within an environment received identical predictions, and any residual per-environment spread in the aggregated CV outputs reflected only differences in the population mean parameter estimates across resampled training folds. This observation exposes the main limitation of purely mechanistic models for breeding, as they cannot be used to rank or select candidate genotypes. Fitting separate models to individual genotypes is feasible, but in the absence of a co-ancestry matrix or marker-based constraint, the algorithm is free to overparameterize and plausibly assign contradictory effects to the same genomic region across genotypes, producing spurious estimates.

At the opposite end of the benchmark spectrum is the plain GBLUP model which relies entirely on the covariance structure estimated from genome-wide markers (Eq. 10). It captures additive genetic variation and accounts for fixed mean differences across environments but provides no mechanism to extrapolate beyond the conditions observed in training, since environments enter the model only as intercepts rather than through their physiological drivers (i.e. temperature and photoperiod). Consequently, GBLUP was considerably less accurate than both CGM-WGP and

RN-GBLUP even under sparse testing scenarios (Table 1), and its accuracy collapsed under new environment scenarios, confirming that purely statistical additive models cannot generalize to novel environments without and explicit representation of GxE.

RN-GBLUP (Jarquín et al. 2014) addresses this limitation by incorporating environmental similarity through covariance kernels constructed from temperature and daylength, and their interactions with the genomic kernel via the Hadamard product (Eq. 9). This formulation captures GxE statistically, allowing predictions to transfer to novel environments provided the target lies within the convex hull of the training kernel space. In our experiments, RN-GBLUP achieved the highest prediction accuracy under sparse testing (beans CV2 $r = 0.93$; broccoli CV2 $r = 0.81$) and remained high when parameters were estimated for new genotype (beans CV1 $r = 0.92$, RMSE = 3.4 d; broccoli CV1 $r = 0.76$, RMSE = 8.1 d). These results are consistent with the design of the algorithm as a flexible statistical smoother over the GxE surface. Its performance deteriorated, however, under new environment scenarios that required extrapolation beyond the training set (beans CV0 $r = 0.76$, RMSE = 6.4 d, driven by large errors at ND, see Figure 6). Wallace et al. (1991) showed that days to flower in beans follows a U-shaped response driven by extreme temperatures. In ND, where genotypes were exposed to long days and high temperatures, and no environments combined long days with low temperatures, this imbalance affected parameter estimation more in RN-GBLUP than in CGM-WGP. Prediction errors in bean could be further reduced by modeling days to flowering with an approach that combines leaf/node production (temperature effect) and the node at which the first flower appears (photoperiod effect)(Wallace et al. 1991).

The CGM-WGP framework differs from RN-GBLUP in how GxE is captured. Rather than learning the interaction surface from kernel similarity, GxE emerges structurally from composition of genotype-specific physiological parameters ($\Theta_g, S_g, P_{c,g}$) with nonlinear temperature and photoperiod response functions (Eqs. 1-4). Two genotypes differing in physiological parameters will exhibit rank changes between different thermal and photoperiod regimes as a direct consequence of the biology encoded in the simulator, without any interaction variance component being fitted. This structural representation captures thresholds and timing effects like the arrest of broccoli inflorescence development above 30°C (Björkman and Pearson 1998), genotype-dependent reversal of photoperiod induced flowering delay in beans (White and Laing 1989), that are difficult to recover from kernel-based GxE decomposition alone. Accordingly, CGM-WGP achieved higher prediction accuracy and lower RMSE than RN-GBLUP under the new environment scenarios (Figure 6) and for new genotypes and new environment scenario (supplementary Figure 4).

Two philosophies exist for integrating genomic information into crop growth models (Messina et al. 2018; Onogi et al. 2016). The two-stage approach estimates CGM parameters per genotype independently and subsequently regresses them on markers via a genomic model such as a GBLUP (Onogi et al. 2016), offering modularity, computational simplicity, and compatibility with any crop model simulator (DSSAT, APSIM, etc.). Its principal limitation is that Stage 1 errors propagate into Stage 2, and genotypes with sparse phenotypic data yield poorly identified parameter estimates that the genomic model cannot rescue. The joint approach embeds the genomic prior directly into the physiological optimization so that markers regularize parameter estimates during fitting and shrink poorly identified genotypes toward their genomic neighbors. Our implementation expands the approach by Messina et al. (2006) by replacing the linear

regression models by genomic selection models and adding an iterative cycle that enables the algorithm to use genomic information to regularize the estimation of CGM parameters (Messina et al. 2018). Our approach is particularly advantageous when per-genotype data are limited, as in breeding programs where candidate lines are rarely evaluated across many environments. For our datasets the joint approach was preferable, and prediction for untested genotypes relied directly on the genomic prior without an intermediate smoothing step.

Rather than framing these approaches as competitors, our results suggest CGM-WGP and RN-GBLUP address complementary prediction scenarios that could be components of ensembles (Cooper et al., 2025; Messina et al., 2025). RN-GBLUP excels when the training set densely covers the GxE space and the target of predictions lies within it, a regime typical of sparse-testing and new variety evaluations within a breeding program. CGM-WGP excels when prediction is required for novel planting windows, climate change scenarios, or untested geographies, where biological extrapolation provides information that statistical similarity cannot. Breeding programs operating across both regimes may benefit from maintaining both tools in their prediction pipeline.

4.3 Whole-genome prediction versus QTL-based dynamic models

The common bean dataset employed in this study has supported a productive sequence of increasingly sophisticated QTL-based dynamic models. Bhakta et al. (2017) established a predictive framework using 12 QTL linked to temperature and photoperiod responses. Wallach et al. (2018) extended this by expressing three parameters of a developmental model as linear functions of QTL, capturing GxE through genotype-specific thermal and photoperiod responses. Vallejos et al. (2022) further refined the formulation using a mixed-effects model with separate

minimum and maximum temperature inputs, epistatic QTL interactions, and an unstructured residual covariance across sites. Although epistatic interactions and GxE could in principle be incorporated when predicting CGM parameters, we consider it preferable to refine the CGM structure iteratively, since breeders can act only on additive genetic variance.

Vallejos et al. (2022) report within-sample performance for their dynamic mixed-effects model on this dataset an $R^2 = 0.911$ and $R^2{}_{adj} = 0.909$, evaluated over 815 (RIL x environment) cells with all data contributing to parameter estimation. These values measure goodness-of-fit rather than predictive accuracy on held-put data and are therefore not directly comparable to the cross-validation accuracies reported in Section 3.3. Under held-out evaluation on the same dataset, CGM-WGP achieves Pearson $r = 0.88$ (RMSE = 4.7 d) when predicting previously unobserved genotypes in trained environments (CV1) and $r = 0.86$ (RMSE = 5.2 d) when predicting trained genotypes in an unobserved environment (CV0). Beyond accuracy, the two classes of model target different inference goals. QTL-based dynamic models, by construction, report the physiological loci that drive genotype-specific physiological parameters and therefore support candidate gene prioritization for downstream functional work. CGM-WGP provides a set of per-genotype physiological parameters across populations and can serve as inputs to subsequent QTL or GWAS analyses. QTL-based dynamic models require an antecedent mapping step that ties the resulting predictive framework to the mapping population in which the QTL were identified; applying the model to a new genetic background requires re-mapping. The CGM-WGP framework replaces this step with a genomic relationship matrix derived from all available markers (Eq. 5), which regularizes genotype parameters through pairwise relatedness rather than through a fixed set of causal loci. To this point, although we have used two biparental populations for this work, the CGM-WGP approach can also be transparently used for training

multiparental populations (e.g., NAM and MAGIC, Gage et al., 2020; Yang et al., 2021) and diversity panels to estimate marker effects for causal loci and thus cover a larger genetic space for inference. The physiological structure of the model is preserved, but the genetic representation generalizes to any population for which markers are available without prior QTL characterization.

4.4 Practical implications for breeding

Three applications are particularly relevant for horticultural breeding. First, cultivar placement: predicted flowering time can be computed across a grid of candidate environments to identify production zones in which the genotype reaches anthesis within a window appropriate for marketable yield (Hu et al., 2021). Second, planting-date optimization: for a fixed environment, varying the sowing date in the simulator identifies windows that minimize exposure to heat stress at anthesis, a critical concern for both broccoli (Björkman and Pearson 1998) and beans (Ofir et al. 1993). Third, CGM-WGP can enable breeders incorporate medium-to-long-range climate projections into selection decisions by improving the expected genetic correlation between the sample of current environments and future target environments(Snowdon et al. 2021; Cooper and Messina 2023; Messina et al. 2023). Fourth, the combination of CGM-WGP for cereals and horticultural crops can enable breeding for cropping systems whereby predictions are made for existing and plausible options and selections are tuned to circularization. For example, predictions for broccoli and sorghum in Florida could be made to create a year round system instead of spring and/or winter broccoli plantings.

Beyond prediction, the per-genotype parameters carry biological meaning. θ_g quantifies the physiological time requirement to flowering, S_g the magnitude and direction of the photoperiod

response, and $P_{c,g}$ the critical photoperiod at which the response is half-saturated. These quantities are candidate inputs to QTL or GWAS analyses targeting the genetic architecture of physiological responses themselves, a potentially more powerful approach than mapping on end-point phenotypes for dissecting complex developmental traits.

4.5 Future Directions

Several extensions of this work merit investigation. First, application of the framework to diversity panels or breeding populations, rather than biparental or RIL populations, would test its performance under more practical allelic and heterogeneity of germplasm in a breeding program. Second, enriching the mechanistic kernel to incorporate soil water balance, nitrogen dynamics, and canopy-level radiation interception to test the performance of the algorithm for complex traits. Third, hybrid formulations that combine CGM-WGP and RN-GBLUP are worth exploring in ensemble configurations (Cooper et al., 2025). In such formulations, RN-GBLUP could model the residuals from CGM-WGP predictions, or the two could be combined in an ensemble (Messina et al. 2025; Cooper et al. 2025; Tomura et al. 2026), pairing the prediction strength of the mechanistic component with the local-smoothing strength of the statistical kernel.

5. Conclusions

This study demonstrates that the CGM-WGP framework generalizes from row crops to horticultural species, providing accurate predictions of time to flowering in broccoli and common bean with different population development strategies, experimental design, and physiological responses to the environment. Joint estimation of genotype-specific physiological parameters under a genomic prior captures GxE structurally, yielding higher prediction accuracy

than RN-GBLUP under novel-environment and novel-genotype scenarios. Our results also underscore that the experimental design considerations for CGM-WGP differ from those of standard genomic selection. While genomic selection benefits primarily from increasing the number of genotypes and replicates within a target environment, CGM-WGP depends on spanning sufficient environmental contrast along each axis the model is meant to extrapolate. Without such contrast, per-genotype parameters on that axis collapse to species-level means, as we observed for photoperiod in both datasets. To avoid this, trials that deliberately sample across thermal gradients, photoperiod regimes, or water regimes, according to the physiological response of interest, allow CGM-WGP to calibrate parameters that transfer to scenarios never directly observed, enabling selection for target environments not yet presented in the breeding program's trial network. For breeding programs operating across diverse production environments and expanding germplasm pools, CGM-WGP provides a modular, interpretable, and deployable framework for predicting phenological responses to the environment from marker data alone.

Author Contributions

M.C. Conceptualization, Methodology, Investigation, Data curation, Software, Writing – original draft. C.D.M. Conceptualization, Methodology, Software, Writing – review & editing. L.J.B. Methodology, Software, Writing – review & editing, D.J -review & editing. C.E.V. Resources, Data curation, Writing – review & editing. All authors read and approved the final manuscript.

References

Alemu A, Åstrand J, Montesinos-López OA, Isidro y Sánchez J, Fernández-Gónzalez J, Tadesse W, Vetukuri RR, Carlsson AS, Ceplitis A, Crossa J, Ortiz R, Chawade A (2024)

Genomic selection in plant breeding: Key factors shaping two decades of progress. Mol Plant 17:552-578. doi:10.1016/j.molp.2024.03.007

Amadeu RR, Garcia AAF, Munoz PR, Ferrão LFV (2023) AGHmatrix: genetic relationship matrices in R. Bioinformatics 39 (7). doi:10.1093/bioinformatics/btad445

Bernardo R, Yu J (2007) Prospects for genomewide selection for quantitative traits in maize. Crop Sci 47:1082-1090

Beyene Y, Semagn K, Mugo S, Tarekegne A, Babu R, Meisel B, Sehabiague P, Makumbi D, Magorokosho C, Oikeh S (2015) Genetic gains in grain yield through genomic selection in eight bi-parental maize populations under drought stress. Crop Sci 55 :154-163

Bhakta MS, Gezan SA, Clavijo Michelangeli JA, Carvalho M, Zhang L, Jones JW, Boote KJ, Correll MJ, Beaver J, Osorno JM, Colbert R, Rao I, Beebe S, Gonzalez A, Ricaurte J, Vallejos CE (2017) A Predictive model for time-to-flowering in the common bean based on QTL and environmental variables. G3 Genes Genomes Genet 7 :3901-3912. doi:10.1534/g3.117.300229

Bhakta MS, Jones VA, Vallejos CE (2015) Punctuated distribution of recombination hotspots and demarcation of pericentromeric regions in phaseolus vulgaris L. PLOS ONE 10 (1):e0116822. doi:10.1371/journal.pone.0116822

Björkman T, Pearson KJ (1998) High temperature arrest of inflorescence development in broccoli (Brassica oleracea var. italica L.). J Exp Bot 49:101-106

Boote KJ, Jones JW, Pickering NB (1996) Potential uses and limitations of crop models. Agron J 88:704-716. doi:10.2134/agronj1996.00021962008800050005x

599 Burgueño J, de los Campos G, Weigel K, Crossa J (2012) Genomic prediction of breeding values
600 when modeling genotype × environment interaction using pedigree and dense molecular
601 markers. Crop Sci 52:707-719. doi:10.2135/cropsci2011.06.0299
602 Byrd RH, Lu P, Nocedal J, Zhu C (1995) A Limited memory algorithm for bound constrained
603 optimization. SIAM J Sci Comp 16:1190-1208. doi:10.1137/0916069
604 Cabrera M, Messina CD (2025) A case for breeding heat-tolerant broccoli. npj Sustain Agric
605 3:53. doi:10.1038/s44264-025-00096-8
606 Camargo LEA, Osborn TC (1996) Mapping loci controlling flowering time in Brassica oleracea.
607 Theor App Genet 92:610-616. doi:10.1007/BF00224565
608 Cammarano D, Taylor MA, Thompson JA, Wright G, Faichney A, Haacker R, Orr A, White PJ
609 (2020) Predicting dates of head initiation and yields of broccoli crops grown throughout
610 Scotland. Eur J Agron 116:126055
611 Cooper M, Gho C, Leafgren R, Tang T, Messina C (2014) Breeding drought-tolerant maize
612 hybrids for the US corn-belt: discovery to product. J Exp Bot 65:6191-6204
613 Cooper M, Messina CD (2023) Breeding crops for drought-affected environments and improved
614 climate resilience. Plant Cell 35:162-186. doi:10.1093/plcell/koac321
615 Cooper M, Technow F, Messina C, Gho C, Totir LR (2016) Use of crop growth models with
616 whole-genome prediction: Application to a maize multienvironment trial. Crop Sci
617 56:2141-2156.
618 Cooper M, Tomura S, Wilkinson MJ, Powell O, Messina CD (2025) Breeding perspectives on
619 tackling trait genome-to-phenome (G2P) dimensionality using ensemble-based genomic
620 prediction. Theor App Genet 138:172. doi:10.1007/s00122-025-04960-6

621 Dempster AP, Laird NM, Rubin DB (1977) Maximum likelihood from incomplete data via the
622 EM algorithm. J Royal Stat Soc Series B (Methodological) 39:1-38
623 Diepenbrock CH, Tang T, Jines M, Technow F, Lira S, Podlich D, Cooper M, Messina C (2022)
624 Can we harness digital technologies and physiology to hasten genetic gain in US maize
625 breeding? Plant Physiol 188:1141–1157. https://doi.org/10.1093/plphys/kiab527
626 Dreisigacker S, Pérez-Rodríguez P, Crespo-Herrera L, Bentley AR, Crossa J (2023) Results from
627 rapid-cycle recurrent genomic selection in spring bread wheat. G3 Genes Genomes Genet
628 13. doi:10.1093/g3journal/jkad025
629 Farnham MW, Bjorkman T (2011) Breeding vegetables adapted to high temperatures: a case
630 study with broccoli. HortScience 46:1093-1097
631 Gage JL, Monier B, Giri A, Buckler ES (2020) Ten years of the maize nested association
632 mapping population: Impact, limitations, and future directions. Plant Cell 32:2083-2093.
633 doi:10.1105/tpc.19.00951
634 Hammer G, Messina C, Wu A, Cooper M (2019) Biological reality and parsimony in crop
635 models—why we need both in crop improvement! in silico Plants 1 (1).
636 doi:10.1093/insilicoplants/diz010
637 Heffner EL, Sorrells ME, Jannink JL (2009) Genomic selection for crop improvement. Crop Sci
638 49:1-12
639 Holzworth DP, Huth NI, deVoil PG, Zurcher EJ, Herrmann NI, McLean G, Chenu K, van
640 Oosterom EJ, Snow V, Murphy C (2014) APSIM–evolution towards a new generation of
641 agricultural systems simulation. Environ Mod & Soft 62:327-350

642 Hoogenboom G, White JW, Messina CD (2004) From genome to crop: integration through
643 simulation modeling. Field Crops Res 90:145-163.
644 doi:https://doi.org/10.1016/j.fcr.2004.07.014
645 Hu P, Chapman SC, Dreisigacker S, Sukumaran S, Reynolds M, Zheng B (2021). Using a gene-
646 based phenology model to identify optimal flowering periods of spring wheat in irrigated
647 mega-environments. J Exp Bot. 72:7203-7218. doi: 10.1093/jxb/erab326.
648 Iniguez-Luy FL, Lukens L, Farnham MW, Amasino RM, Osborn TC (2009) Development of
649 public immortal mapping populations, molecular markers and linkage maps for rapid
650 cycling Brassica rapa and B. oleracea. Theor App Genet 120:31-43. doi:10.1007/s00122-
651 009-1157-4
652 Jarquin D, Howard R, Crossa J, Beyene Y, Gowda M, Martini JWR, Covarrubias Pazaran G,
653 Burgueño J, Pacheco A, Grondona M, Wimmer V, Prasanna BM (2020) Genomic
654 prediction enhanced sparse testing for multi-environment trials. G3 (Bethesda) 10
655 (8):2725-2739. doi:10.1534/g3.120.401349
656 Jarquín D, Crossa J, Lacaze X, Du Cheyron P, Daucourt J, Lorgeou J, Piraux F, Guerreiro L,
657 Pérez P, Calus M, Burgueño J, de los Campos G (2014) A reaction norm model for
658 genomic selection using high-dimensional genomic and environmental data. Theor App
659 Genet 127:595-607. doi:10.1007/s00122-013-2243-1
660 Jones JW, Hoogenboom G, Porter CH, Boote KJ, Batchelor WD, Hunt LA, Wilkens PW, Singh
661 U, Gijsman AJ, Ritchie JT (2003) The DSSAT cropping system model. Eur J Agron
662 18:235-265. doi:https://doi.org/10.1016/S1161-0301(02)00107-7

663 Kim S, Kim S, Kiniry JR, Ku K-M (2021) A hybrid decision tool for optimizing broccoli
664 production in a changing climate. Hort Environ Biotech 62:299-312. doi:10.1007/s13580-
665 020-00317-8
666 Lin CW, Fu SF, Liu YJ, Chen CC, Chang CH, Yang YW, Huang HJ (2019) Analysis of ambient
667 temperature-responsive transcriptome in shoot apical meristem of heat-tolerant and heat-
668 sensitive broccoli inbred lines during floral head formation. BMC Plant Biol 19 (1):3.
669 doi:10.1186/s12870-018-1613-x
670 Lin YR, Lee JY, Tseng MC, Lee CY, Shen CH, Wang CS, Liou CC, Shuang LS, Paterson AH,
671 Hwu KK (2018) Subtropical adaptation of a temperate plant (Brassica oleracea var.
672 italica) utilizes non-vernalization-responsive QTLs. Sci Rep 8 (1):13609.
673 doi:10.1038/s41598-018-31987-1
674 Lindemann-Zutz K, Fricke A, Stützel H (2016) Prediction of time to harvest and its variability in
675 broccoli (Brassica oleracea var. italica) Part I. Plant developmental variation and forecast
676 of time to head induction. Sci Hortic 198:424-433.
677 doi:https://doi.org/10.1016/j.scienta.2015.12.023
678 Messina CD, Borras L, Tang T, Cooper M (2023a) Crop improvement can accelerate agriculture
679 adaptation to societal demands and climate change. bioRxiv:2023.2009.2019.558447.
680 doi:10.1101/2023.09.19.558447
681 Messina C, Garcia-Abadillo J, Powell O, Tomura S, Zare A, Ganapathysubramanian B, Cooper
682 M (2025) Toward a general framework for AI-enabled prediction in crop improvement.
683 Theor App Genet 138:151. doi:10.1007/s00122-025-04928-6

Messina CD, Gho C, Hammer GL, Tang T, Cooper M (2023b) Two decades of harnessing standing genetic variation for physiological traits to improve drought tolerance in maize. J Exp Bot 74:4847–4861. https://doi.org/10.1093/jxb/erad231

Messina CD, Jones JW, Boote KJ, Vallejos CE (2006) A gene-based model to simulate soybean development and yield responses to environment. Crop Sci 46:456-466. doi:https://doi.org/10.2135/cropsci2005.04-0372

Messina CD, Sinclair TR, Hammer GL, Curan D, Thompson J, Oler Z, Gho C, Cooper M (2015) Limited-transpiration trait may increase maize drought tolerance in the US corn belt. Agron J 107:1978-1986. doi:https://doi.org/10.2134/agronj15.0016

Messina CD, Technow F, Tang T, Totir R, Gho C, Cooper M (2018) Leveraging biological insight and environmental variation to improve phenotypic prediction: Integrating crop growth models (CGM) with whole genome prediction (WGP). Eur J Agron 100:151-162. doi:https://doi.org/10.1016/j.eja.2018.01.007

Meuwissen THE, Hayes BJ, Goddard ME (2001) Prediction of total genetic value using genome-wide dense marker maps. Genet 157:1819-1829. doi:10.1093/genetics/157.4.1819

Monterroso VA, Wien HC (1990) Flower and pod abscission due to heat stress in beans. J Am Soc Horti Sci 115:631-634

Ofir M, Gross Y, Bangerth F, Kigel J (1993) High temperature effects on pod and seed production as related to hormone levels and abscission of reproductive structures in common bean (Phaseolus vulgaris L.). Sci Hortic 55:201-211. doi:https://doi.org/10.1016/0304-4238(93)90032-L

Okazaki K, Sakamoto K, Kikuchi R, Saito A, Togashi E, Kuginuki Y, Matsumoto S, Hirai M (2007) Mapping and characterization of FLC homologs and QTL analysis of flowering

time in Brassica oleracea. Theor App Genet 114:595-608. doi:10.1007/s00122-006-0460-6

Olesen JE, Grevsen K (1997) Effects of temperature and irradiance on vegetative growth of cauliflower (Brassica oleracea L. botrytis) and broccoli (Brassica oleracea L. italica). J Exp Bot 48:1591-1598

Onogi A, Watanabe M, Mochizuki T, Hayashi T, Nakagawa H, Hasegawa T, Iwata H (2016) Toward integration of genomic selection with crop modelling: the development of an integrated approach to predicting rice heading dates. Theor App Genet 129:805-817. doi:10.1007/s00122-016-2667-5

Peksen E (2007) Dynamics of flower appearance, flowering, pod and seed setting performance and their relations to seed yield in common bean (Phaseolus vulgaris L.). Pakistan J Bot 39:485-496

Shu J, Liu Y, Zhang L, Li Z, Fang Z, Yang L, Zhuang M, Zhang Y, Lv H (2018) QTL-seq for rapid identification of candidate genes for flowering time in broccoli × cabbage. Theor App Genet 131:917-928. doi:10.1007/s00122-017-3047-5

Siomos AS, Koularmanis K, Tsouvaltzis P (2022) The impacts of the emerging climate change on broccoli (Brassica oleracea L. var. italica Plenck.) Crop Hortic 8 (11):1032

Snowdon RJ, Wittkop B, Chen T-W, Stahl A (2021) Crop adaptation to climate change as a consequence of long-term breeding. Theor App Genet 134:1613-1623. doi:10.1007/s00122-020-03729-3

Stansell Z, Farnham M, Björkman T (2019) Complex horticultural quality traits in broccoli are illuminated by evaluation of the immortal BolTBDH mapping population. Front Plant Sci 10:1104

730 Tan D, Birch C, Wearing A, Rickert K (2000a) Predicting broccoli development I. Development
731 is predominantly determined by temperature rather than photoperiod. Sci Hortic 84:227-
732 243
733 Tan DKY, Wearing AH, Rickert KG, Birch CJ (2000b) Broccoli yield and quality can be
734 determined by cultivar and temperature but not photoperiod in south-east Queensland.
735 Aust J Exp Agric 39:901-909. doi:https://doi.org/10.1071/EA99053
736 Technow F, Messina CD, Totir LR, Cooper M (2015) Integrating crop growth models with
737 whole genome prediction through approximate bayesian computation. PLoS One 10
738 (6):e0130855. doi:10.1371/journal.pone.0130855
739 Tomura S, Powell O, Wilkinson MJ, Cooper M (2026) Ensemble-based genomic prediction for
740 maize flowering time improves prediction accuracy and reveals novel insights into trait
741 genetic variation. G3 Genes Genomes Genet. doi:10.1093/g3journal/jkag090
742 Vallejos CE, Jones JW, Bhakta MS, Gezan SA, Correll MJ (2022) Dynamic QTL-based
743 ecophysiological models to predict phenotype from genotype and environment data.
744 BMC Plant Biol 22 (1):275. doi:10.1186/s12870-022-03624-7
745 VanRaden PM (2008) Efficient methods to compute genomic predictions. J Dairy Sci 91:4414-
746 4423. doi:10.3168/jds.2007-0980
747 Wallace DH, Gniffke PA, Masaya PN, Zobel RW (1991) Photoperiod, temperature, and
748 interaction effects on days and nodes required for flowering of bean. J Am Soc Hortic Sci
749 116:534-543. doi:10.21273/JASHS.116.3.534
750 Wallach D, Hwang C, Correll MJ, Jones JW, Boote K, Hoogenboom G, Gezan S, Bhakta M,
751 Vallejos CE (2018) A dynamic model with QTL covariables for predicting flowering

time of common bean (Phaseolus vulgaris) genotypes. Eur J Agron 101:200-209. doi:https://doi.org/10.1016/j.eja.2018.10.003

White JW, Laing DR (1989) Photoperiod response of flowering in diverse genotypes of common bean (Phaseolus vulgaris). Field Crops Res 22:113-128. doi:https://doi.org/10.1016/0378-4290(89)90062-2

Wurr D, Fellows J, Phelps K, Reader R (1995) Vernalization in calabrese (Brassica oleracea var. italica)-a model for apex development. J Experimental Botany 46:1487-1496

Yang CJ, Edmondson RN, Piepho H-P, Powell W, Mackay I (2021) Crafting for a better MAGIC: systematic design and test for multiparental advanced generation inter-cross population. G3 Genes Genomes Genet 11. doi:10.1093/g3journal/jkab295

Statements and Declarations

The authors have no relevant financial or non-financial interests to disclose

Funding

This material is based upon work supported by the National Science Foundation Graduate Research Fellowship under Grant No. DGE-2236414. Any opinions, findings, and conclusions or recommendations expressed in this material are those of the author(s) and do not necessarily reflect the views of the National Science Foundation. U.S. Government, Department of State under the terms of Cooperative Agreement No. 7200AA23LE00003

Data Availability

The datasets and scripts generated during and for the analysis during the current study are available from the corresponding author on reasonable request.

Figure captions

Fig 1 Daily environmental conditions for six broccoli plantings at the University of Florida Hastings Agricultural Extension Center (HAEC) (**A**), and five environments evaluated in the bean experiments (**B**). Data were obtained from the Florida Automated Weather Network (FAWN) and (Vallejos et al. 2022; Wallach et al. 2018; Bhakta et al. 2017). Panels show daily maximum (red) and minimum (blue) air temperatures (°C), with a dashed line indicating the 30°C threshold for heat stress in broccoli, and daily solar radiation (black) measured at 2 m height (W/m²)

Fig 2 Architecture of the CGM-WGP framework. It couples a mechanistic model of daily development with a genomic prior on per-genotype parameters and jointly fits by alternating optimization

Fig 3 Distribution of flowering dates for (A) the bean RIL population evaluated in five environments and (B) individuals in the BolTBDH broccoli population across six planting dates, visualized as violin plots

Fig 4 Per-genotype physiological time requirement Θ_g extracted from the CGM-WGP model, averaged across folds (beans n = 187, broccoli n= 186)

Fig 5 Method ranking across the four cross-validation scenarios for beans and broccoli. Rank is by Pearson r per scenario (1 = best); vertical error bars encode RMSE magnitude

Fig 6 Observed vs predicted days to anthesis under leave-one-environment-out cross validation (CV0) for beans (top), and broccoli (bottom), across RN-GBLUP (left) and CGM-WGP (right) models. Each point is a (genotype, environment) cell from the held-out environment

Supplementary Fig 1 Genomic relationship matrix for the BolTBDH broccoli population (n = 200)

Supplementary Fig 2 Genomic relationship matrix for the Calima × Jamapa bean RIL family (n = 188)

Supplementary Fig 3 AMMI biplots characterizing genotype-by-environment interaction in broccoli and bean flowering time

Supplementary Fig 4 Observed versus predicted days to anthesis under the new-genotype × new-environment (CV00) cross-validation scheme

Tables

Table 1 Prediction accuracy (*r*) and RMSE (days) for four tested models across validation schemes in beans and broccoli. Sparse testing (CV2), new genotype (CV1), new environment (CV0), new genotype and new environment (CV00). NA indicate the mechanistic CGM baseline, which has no per-genotype parametrization and is therefore degenerate for CV1 and CV00. Values are averages over five folds

Scheme	Metric	Prediction methodology			
		CGM	GBLUP	RN-GBLUP	CGM-WGP
			Beans		
CV2	*r*	0.83	0.34	0.93	0.90
	RMSE	7.5	8.5	3.2	4.7
CV1	*r*	NA	0.32	0.92	0.88
	RMSE	NA	8.5	3.4	4.7
CV0	*r*	0.77	−0.55	0.76	0.86
	RMSE	9.4	10.1	6.4	5.2
CV00	*r*	NA	−0.64	0.79	0.83
	RMSE	NA	10.1	6.3	5.4
			Broccoli		
CV2	*r*	0.42	0.37	0.81	0.68
	RMSE	14.2	11.8	7.4	9.1

CV1	*r*	NA	0.35	0.76	0.64
	RMSE	NA	12.0	8.1	9.6
CV0	*r*	0.49	−0.13	0.58	0.66
	RMSE	12.7	12.8	10.6	9.4
CV00	*r*	NA	−0.20	0.52	0.65
	RMSE	NA	12.8	11.5	9.4

810

811

Figures

Fig 1

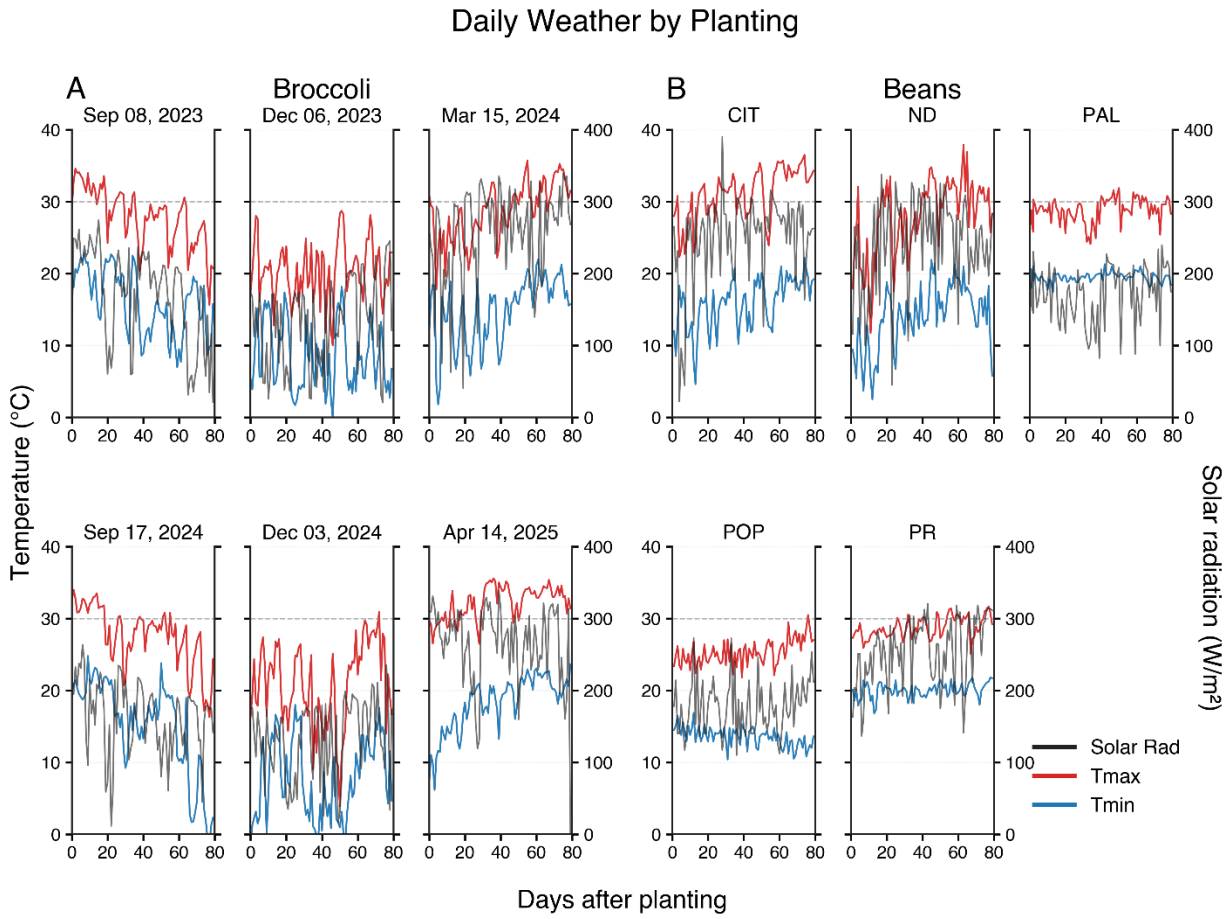

Fig 2

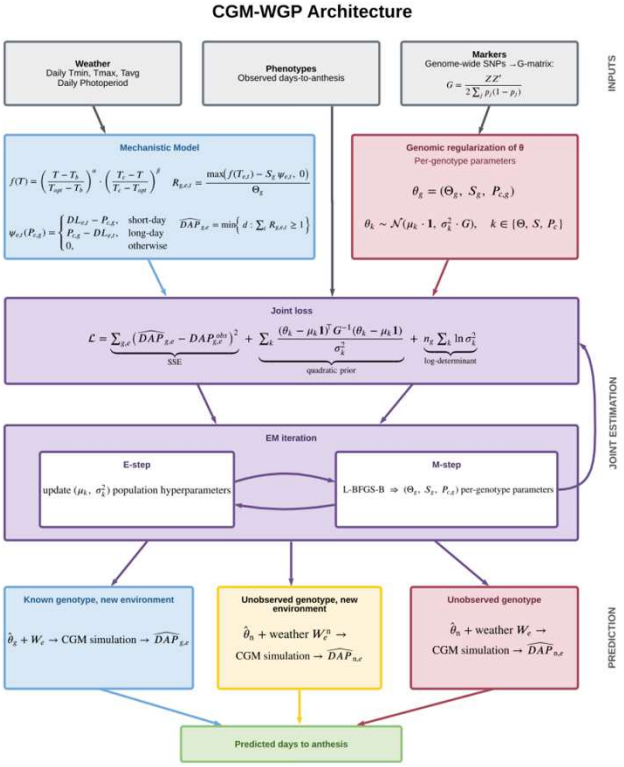
CGM-WGP Architecture
Weather
Daily Tmin, Tmax, Tavg
Daily Photoperiod
Phenotypes
Observed days-to-anthesis
Markers
Genome-wide SNPs → G-matrix:
INPUTS
Mechanistic Model
Genomic regularization of θ
Per-genotype parameters
Joint loss
SSE
quadratic prior
log-determinant
JOINT ESTIMATION
EM iteration
E-step
update (μ_k, σ_k²) population hyperparameters
M-step
L-BFGS-B ⇒ (Θ_g, S_g, P_{c,g}) per-genotype parameters
Known genotype, new environment
Unobserved genotype, new environment
Unobserved genotype
PREDICTION
Predicted days to anthesis

819 **Fig 3**

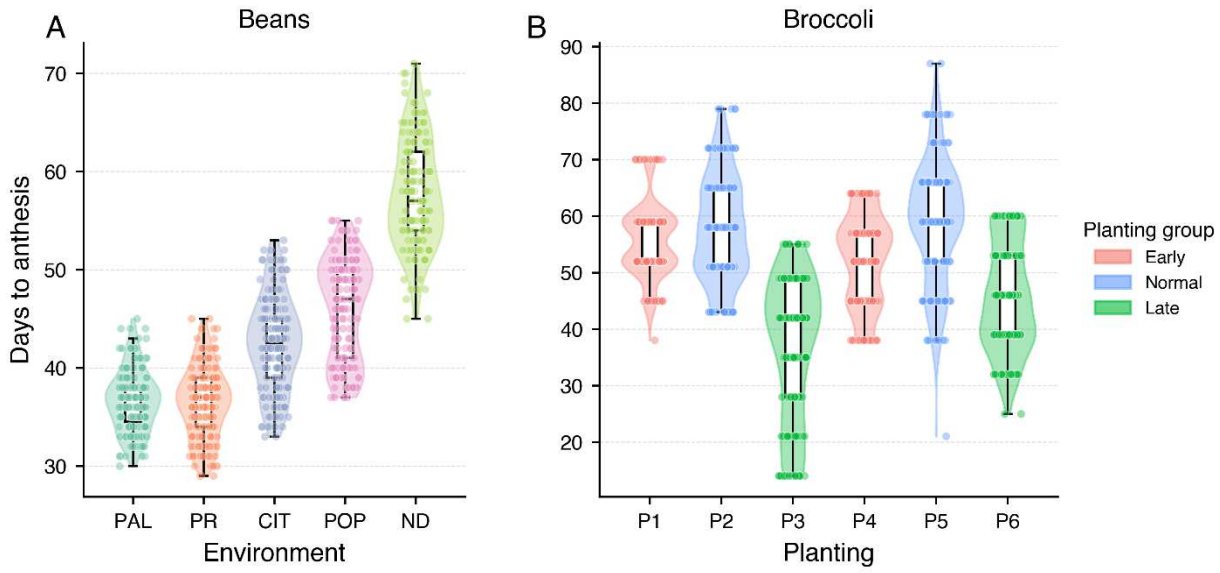

820

821

822 **Fig 4**

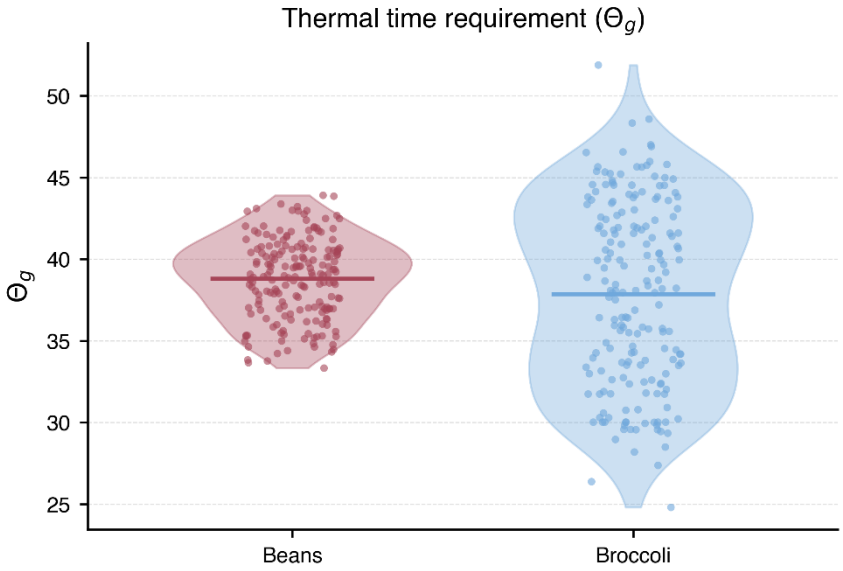

823

824

Fig 5

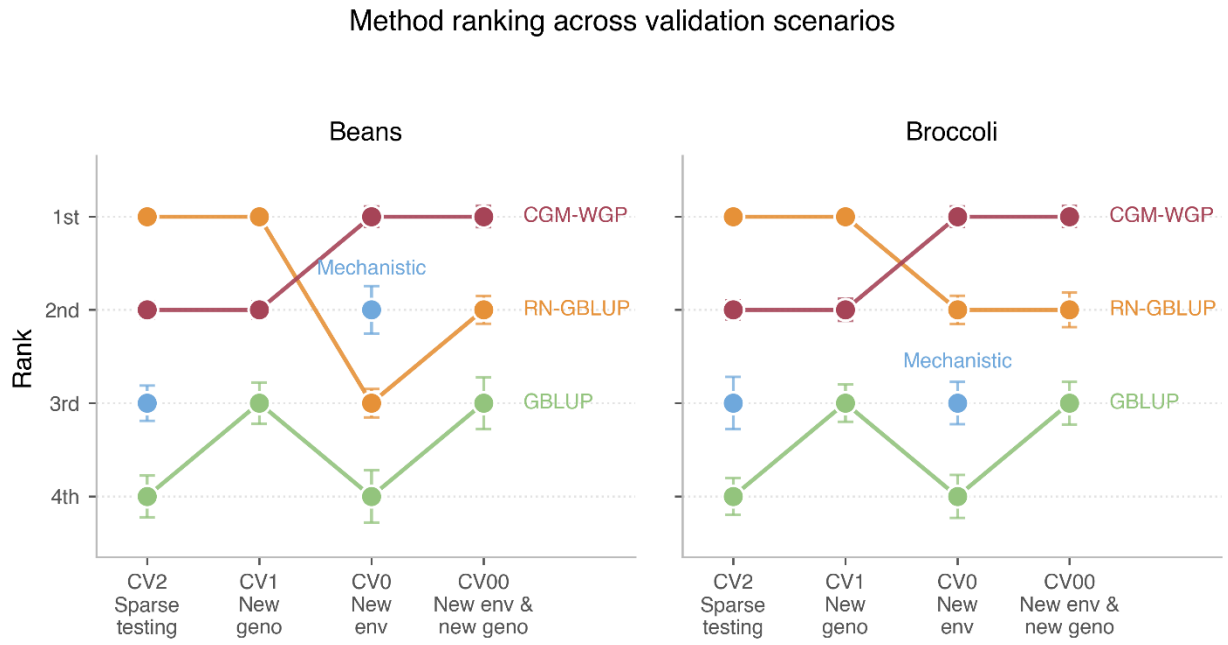
Method ranking across validation scenarios
Beans
Broccoli
Rank
1st
2nd
3rd
4th
CGM-WGP
RN-GBLUP
Mechanistic
GBLUP
CV2 Sparse testing
CV1 New geno
CV0 New env
CV00 New env & new geno

828 **Fig 6**

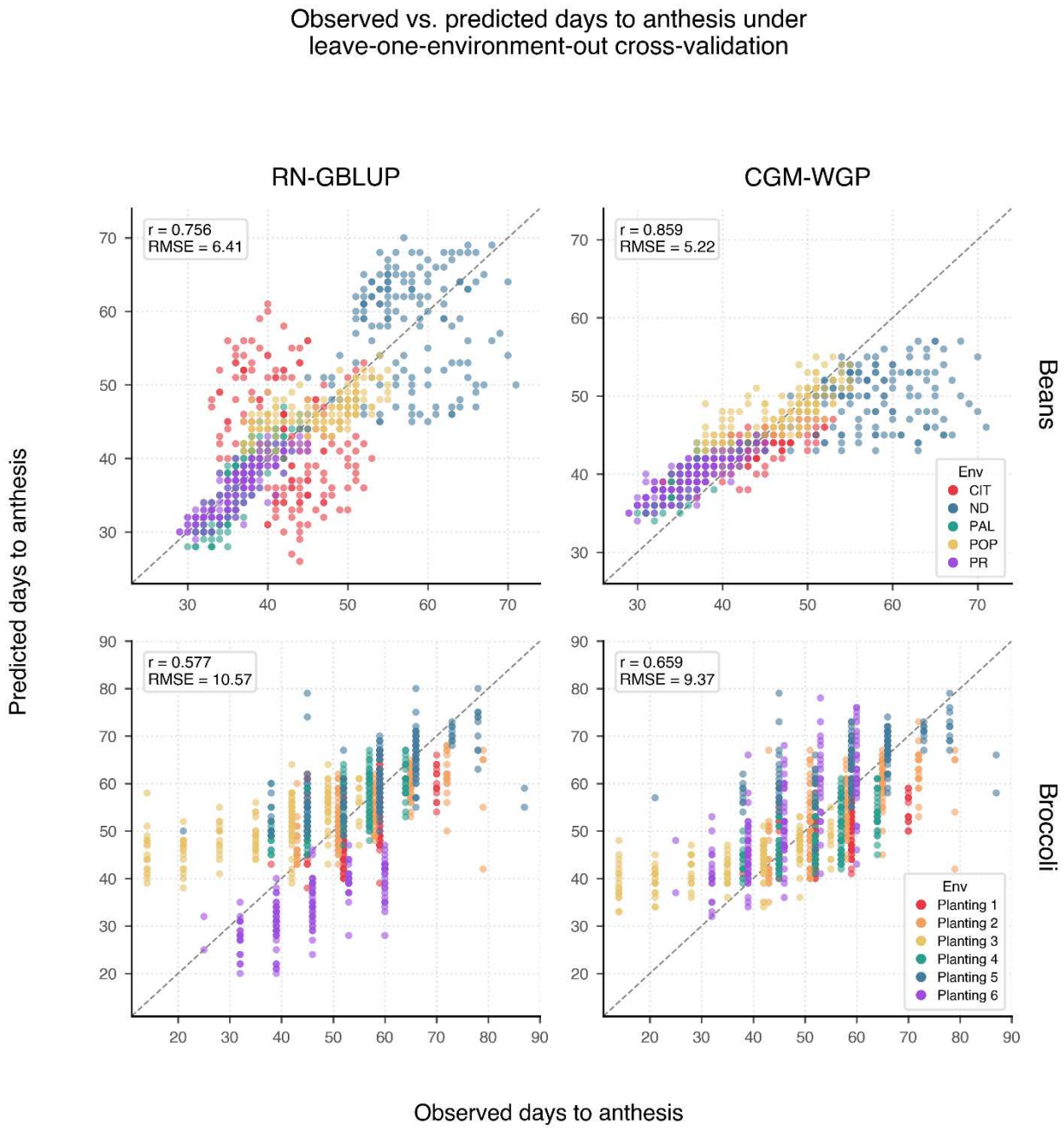

829

830

Supplementary Fig 1

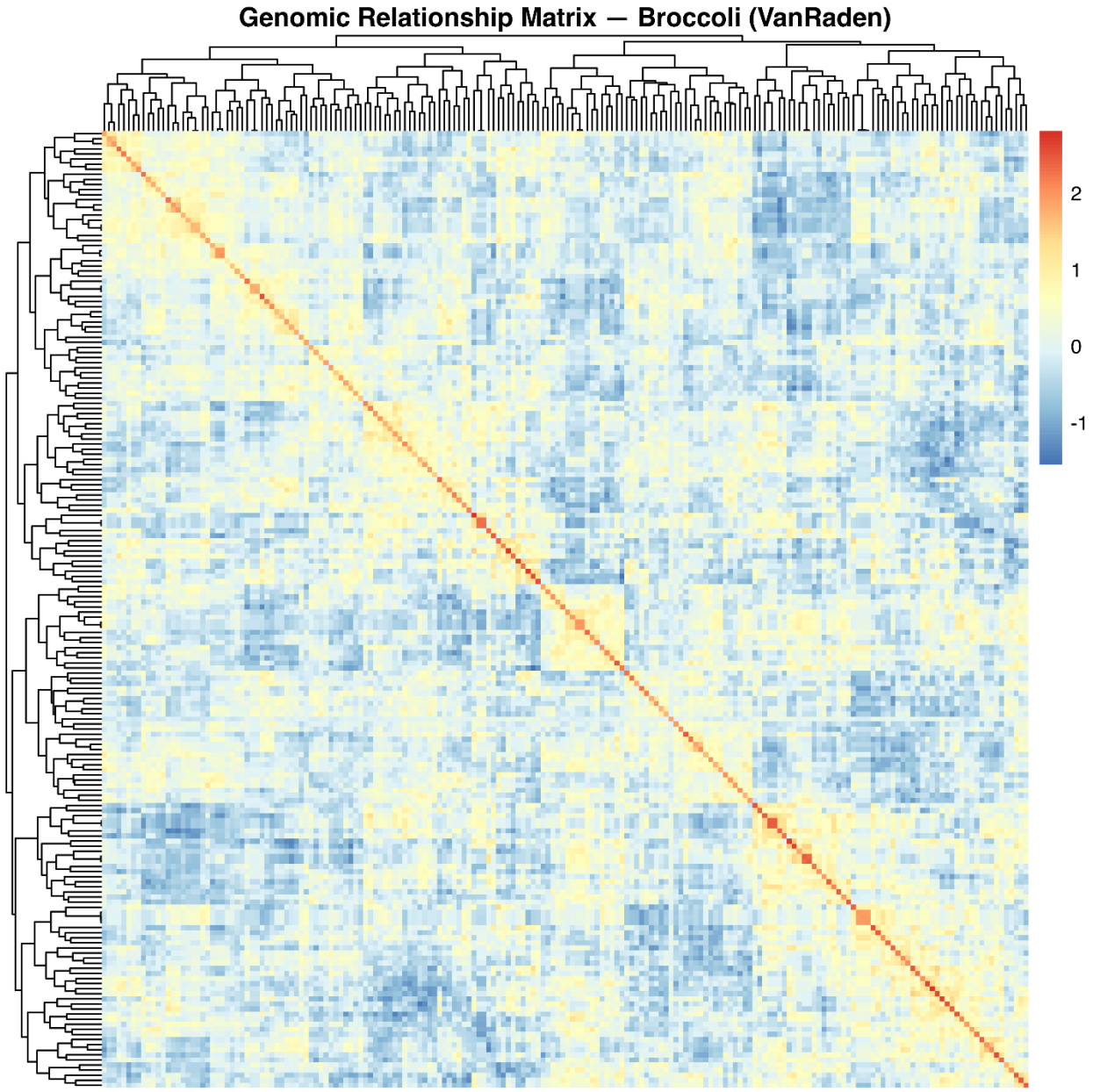

Supplementary Fig 2

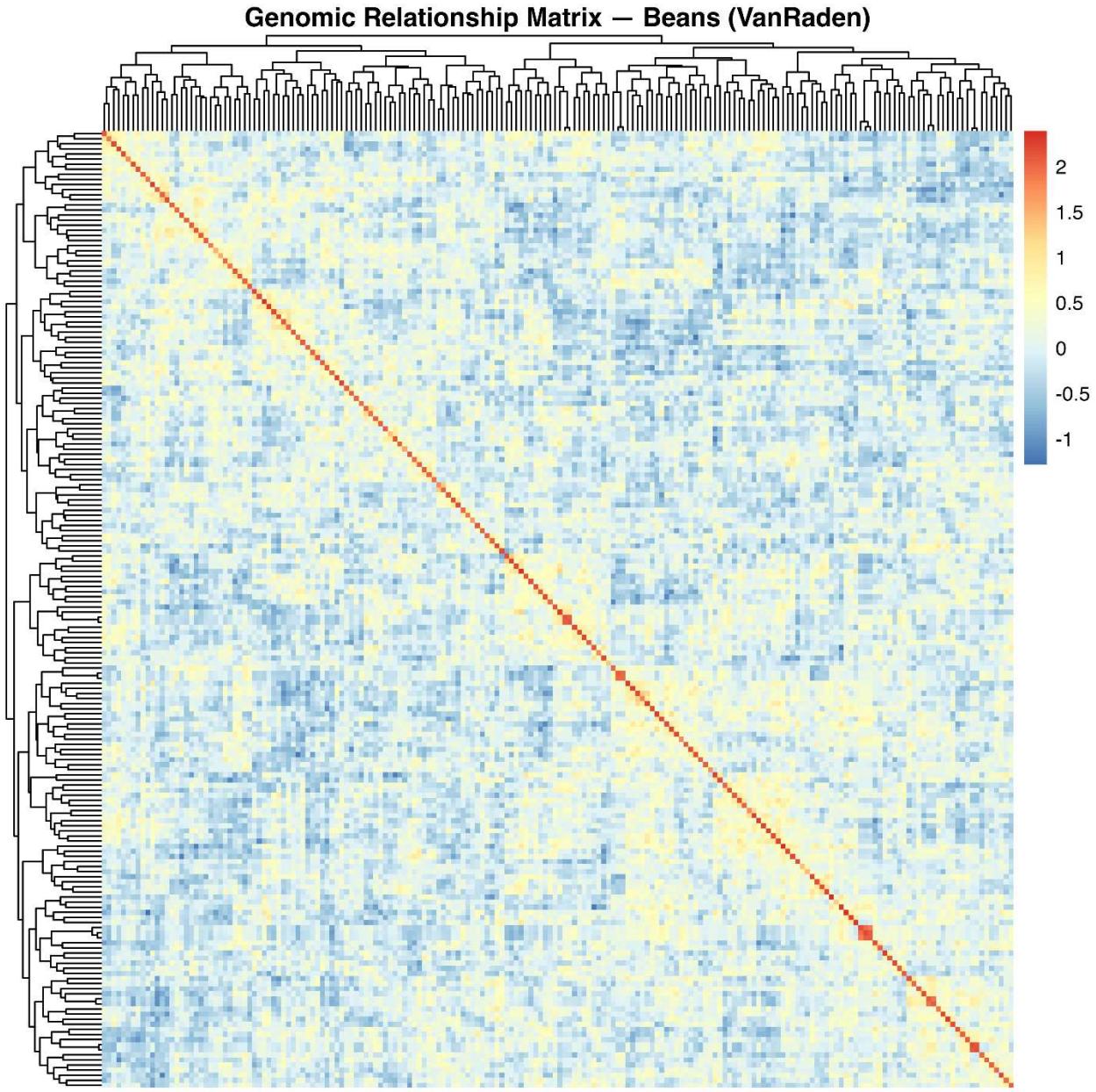

Supplementary Fig 3

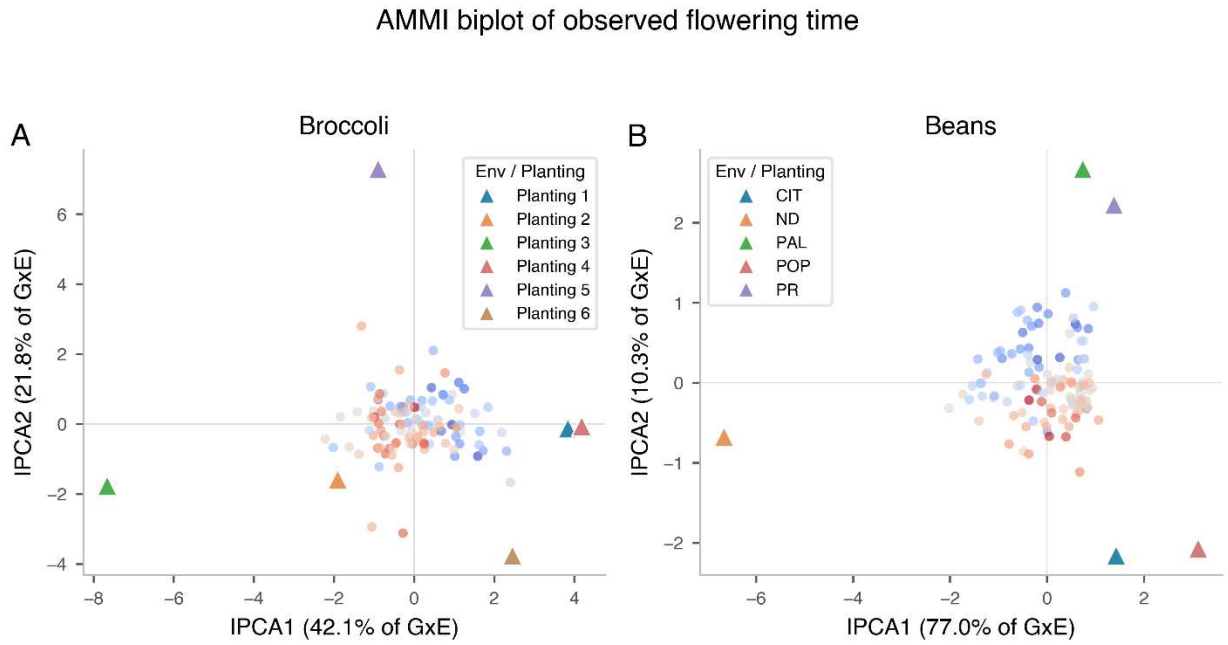

Supplementary Fig 4